

Monte Carlo Studies of Helicity Modulus and Heat Capacity of a Coupled XY Model in Two Dimensions

I. M. Jiang,¹ T. Stoebe,² and C. C. Huang^{3,*}

¹*Department of Physics, National Sun Yat-sen University, Kaohsiung, Taiwan*

²*Department of Chemical Engineering and Materials Science, University of Minnesota, Minneapolis, Minnesota 55455*

³*School of Physics and Astronomy, University of Minnesota, Minneapolis, Minnesota 55455*

(Received 21 July 1995)

Utilizing Monte Carlo simulation techniques, we have calculated both the helicity modulus and heat capacity versus temperature of a coupled classical XY model in two dimensions. Our model system is based on a Hamiltonian first proposed by Bruinsma and Aeppli [Phys. Rev. Lett. **48**, 1625 (1982)]. The helicity modulus results strengthen our previous report of a new type of phase transition in which two distinct types of order are simultaneously established through a single continuous transition.

PACS numbers: 61.30.-v, 64.60.-i, 64.70.Md

We have recently performed simultaneous measurement of both the heat capacity and optical reflectivity near the smectic-A (SmA) to hexatic-B (HexB) transition of extremely thin free-standing 3(10)OBC liquid-crystal films [1]. 3(10)OBC is a member of the *nmOBC* (*n*-alkyl-4'-*n*-alkoxy-biphenyl-4-carboxylate) homologous series. The films are layered structures, and the layers are separated by roughly the length of the sample molecules ($\approx 25 \text{ \AA}$). This work has revealed the following salient results: (1) Unlike thicker films ($N > 2$), two-layer ($N = 2$) films display only a single heat-capacity anomaly, indicating that the two-layer films have reached the two-dimensional (2D) limit. (2) To within the high resolution (about 2 parts in 10^5) of our measurement, the optical-reflectivity data display a smooth variation through the SmA-HexB transition with an inflection point located within 10 mK of the peak position of the heat-capacity anomaly. No jump in the optical reflectivity data can be resolved to within the 2 mK temperature resolution of this measurement [2]. These results indicate that the liquid-hexatic transition in two-layer films is continuous. (3) Both heat-capacity and optical-reflectivity data can be well described by a power law expression with heat-capacity critical exponent $\alpha = 0.31 \pm 0.03$ [3]. If the liquid-hexatic transition in two-layer 3(10)OBC films exhibits an XY-like transition as two-dimensional melting theory suggests [4,5], these three experimental findings clearly indicate that hexatic order may not be the only order parameter responsible for the SmA-HexB transition in 3(10)OBC. The existence of the herringbone order in the HexB phase has recently been demonstrated by electron diffraction studies from an overexposed eight-layer 3(10)OBC film [6]. Inspired by the above experimental findings, we have conducted computer simulations to gain further physical insight into the nature of coupled-order systems [7] which have been found in various physical systems.

In light of x-ray [8] and calorimetric [9] studies of bulk samples near the SmA-HexB transition of 65OBC,

Bruinsma and Aeppli [10] proposed a Hamiltonian to describe this intriguing transition in three dimensions. The basic idea is the following: The bond-orientational order (Ψ) can be represented by an XY order parameter [$\Psi = |\Psi| \exp(i6\psi)$] [4]. Because the HexB phase exhibits only short ranged positional order, they suggested that the herringbone order (Φ) could also be represented by an XY order parameter [$\Phi = |\Phi| \exp(i2\phi)$] [11]. To formulate the Landau free energy which describes both the hexatic and herringbone order, one notices that the hexatic order possesses sixfold symmetry, while rotating a herringbone pattern by 180° leaves it unchanged. Thus the coupling term should be invariant under the transformations $\psi \rightarrow \psi + m(\pi/3)$ and $\phi \rightarrow \phi + n\pi$, where m and n are integers. Bruinsma and Aeppli included such a coupling term and considered the fluctuation-induced corrections to mean-field behavior in three dimensions. Their results demonstrate the existence of two tricritical points [10]. The corrections to mean-field behavior associated with the proximity of a tricritical point could potentially account for the large heat-capacity critical exponents observed near the SmA-HexB transition. However, while this argument is plausible, it is extremely difficult to understand why seven different *nmOBC* compounds and five binary mixtures, with very different SmA and HexB temperature ranges, yield such similar values ($\alpha = 0.60$) [12] and appear to be equally affected by such a special thermodynamic point [13].

To lowest order in Ψ and Φ , the simplified Hamiltonian on a two-dimensional lattice can be written as

$$H = -J_1 \sum_{\langle i,j \rangle} \cos(\psi_i - \psi_j) - J_2 \sum_{\langle i,j \rangle} \cos(\phi_i - \phi_j) - J_3 \sum_i \cos(\psi_i - 3\phi_i), \quad (1)$$

where the coefficients J_1 and J_2 are the nearest-neighbor ($\langle i, j \rangle$) coupling constants for the bond-orientational (Ψ) and herringbone order (Φ), respectively. The coefficient J_3 determines the coupling strength between these two

types of order at the same lattice site. We are interested in situations in which Ψ and Φ are coupled relatively strongly, and therefore J_3 was always taken to be larger than both J_1 and J_2 ($J_3 = 2.1$) for all of the work presented here.

Employing standard Monte Carlo techniques [14], we have conducted detailed heat-capacity calculations on a 30×30 lattice for $J_3 = 2.1$, $J_1 = 1.0$, and various values of J_2 . The schematic phase diagram obtained previously from the peak positions of the heat-capacity anomalies is shown in Fig. 1 [15]. For sufficiently low values of J_2 , the sequence of isotropic-hexatic-hexatic-herringbone transitions can be easily identified. For example, Fig. 2 displays the simulation results for the case of $J_2 = 0.3$. The heat-capacity data exhibit a broad hump just above $T = 1.0$ which is followed by a sharp heat-capacity anomaly near $T = 0.43$ (an order-disorder transition). The hump represents a defect-mediated 2D XY transition. The peak denotes a three-state Potts transition and is characterized by a heat-capacity critical exponent $\alpha = 0.36 \pm 0.05$ [15]. An interesting region of parameter space is encountered for $J_2 > 0.75$ as the isotropic to the hexatic-herringbone phase transition appears to be characterized by a single anomaly [15]. Detailed simulations yield continuous, sharp heat-capacity anomalies for $0.75 < J_2 < 1.4$ [15]. Furthermore, these sharp anomalies can be described by a power law with critical exponent $\alpha = 0.36 \pm 0.05$ which is in reasonably good agreement with our two-layer film results from five nmOBC compounds. Similar behavior has been reported in the 2D systems showing the compe-

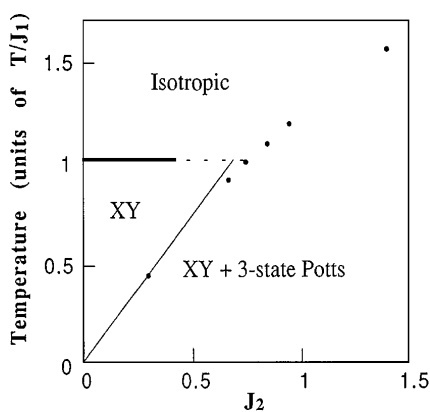


FIG. 1. Schematic of the phase diagram obtained from simulation results of heat capacity [15]: transition temperature versus J_2 with $J_1 = 1.0$ and $J_3 = 2.1$. The solid dots are determined by the peak positions of heat-capacity anomalies. The narrow line is determined by the relationship $T_{c2} = 3J_2/2$ [24]. The heavy isotropic-XY transition line is assumed to be at $T = 1.0$. But as the temperature range for the XY state diminishes, it is very difficult to separate the small heat-capacity hump for the XY transition from the large heat-capacity peak associated with the three-state Potts transition. We have therefore used a dashed line in this region to indicate this uncertainty.

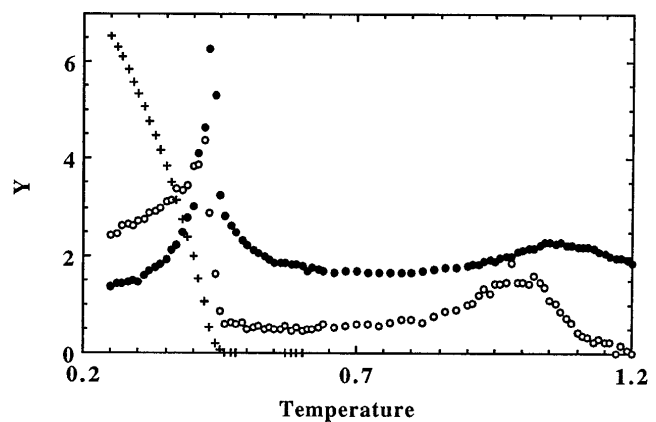


FIG. 2. Temperature dependence of the heat capacity (C_v , solid dots), the energy difference ($\Delta U/2$, open circles) and helicity modulus ($\gamma/2$, crosses) for $J_1 = 1.0$, $J_2 = 0.3$, and $J_3 = 2.1$ from a 30×30 lattice.

tion between the Kosterlitz-Thouless-type and Ising-type transitions [7]. Our previous heat-capacity simulations provided the same critical exponent for the hexatic-hexatic-herringbone and isotropic-hexatic-herringbone transitions; however, the helicity modulus results now enable these transitions to be distinguished.

An independent method of locating the transition temperature and investigating the nature of transition relies on calculated values for the helicity modulus, an elegant concept introduced by Fisher, Barber, and Jasnow [16]. The helicity modulus is related to the difference in Helmholtz free energy obtained by applying periodic and twisted boundary conditions, namely,

$$F(\omega) - F(0) = 2\gamma(\beta)\omega^2, \quad (2)$$

This expression represents a twist of phase angle ω applied along one axis of an $N \times N$ lattice. The coefficient $\gamma(\beta)$ describes the temperature ($\beta = 1/T$) dependence of the helicity modulus and is a measure of the rigidity of the system under an imposed phase twist. It is interesting to note a clever argument that relates γ to the superfluid density in liquid helium [16,17]. Thus the calculation of γ becomes an important method to characterize not only the XY model [18–20] but also a related model [21] in two dimensions.

On the basis of this definition, the difference between the internal energy obtained under periodic boundary conditions $\langle U_p \rangle$ and antiperiodic ($\omega = \pi$) boundary conditions $\langle U_a \rangle$ yields the derivative of the helicity modulus [16], namely,

$$\{d[\beta\gamma(\beta)]/d\beta\}/2 = (\langle U_a \rangle - \langle U_p \rangle)/\pi^2. \quad (3)$$

To further investigate the nature of the single heat-capacity peak obtained in our simulations using $0.75 < J_2 < 1.4$ (with $J_1 = 1.0$, $J_3 = 2.1$), we have performed helicity calculations on a 30×30 lattice employing the coupled XY Hamiltonian presented as Eq. (1). The work

has been tested in the simple XY model [17] as well as in an intuitively apparent region, namely, $J_1 = 1.0$, $J_2 = 0.3$, and $J_3 = 2.1$. The calculated internal energies obtained by applying periodic and antiperiodic boundary conditions provide both heat capacity (C_v) and $\{d[\beta\gamma(\beta)]/d\beta\}/2$ data. The antiperiodic boundary conditions were imposed on both variables ψ and ϕ along only one of the 2D lattice axes. The results after performing 500 000 Monte Carlo steps (MCS) are shown in Fig. 2. Such a large number of MCS were found to be necessary to achieve reasonable statistics for the values of $\{d[\beta\gamma(\beta)]/d\beta\}/2$ as the values for $\langle U_p \rangle$ and $\langle U_a \rangle$ generally differ by less than 1%. The heat-capacity data yield the expected result [15], a defect-mediated XY transition around $T = 1$ followed by an order-disorder-type three-state Potts transition near $T = 0.43$. The energy difference $[\Delta U = (\langle U_a \rangle - \langle U_p \rangle)/\pi^2]$ provides distinct features associated with these two very different phase transitions. At sufficiently high temperatures, the imposed antiperiodic boundary condition does not change the internal energy. Thus $\Delta U = 0$ for $T > 1.16$. Near the 2D XY transition, both heat capacity and the difference in internal energy (ΔU) yield broad humps with maxima located near $T = 1.07$ and 0.98 , respectively. The peak position of the ΔU data more closely represents the reported defect-mediated transition temperature [22].

In the vicinity of the order-disorder transition (where ϕ becomes ordered), while the heat capacity displays a fairly symmetric peak, the ΔU data exhibit a sharp rise followed by a gradual decrease upon decreasing temperature. The sharp rise in ΔU coincides with the heat-capacity peak position at $T = 0.43$. Between the two transitions, $0.46 < T < 0.6$, the ΔU data are relatively constant and nonzero, reflecting the ψ order. After subtracting this residual difference, we can calculate the helicity modulus (γ) for $T < 0.6$ due to the order of ϕ (see Fig. 2). As expected, near the order-disorder transition, $\gamma \rightarrow 0$ as $T \rightarrow T_c^-$ and $\gamma = 0$ for $T > T_c$. The helicity data presented in Fig. 2 could be successfully fit by a simple power law expression, $\gamma = \gamma_0[(T - T_c)/T_c]^{-\nu}$, yielding the critical exponent $\nu = 0.40 \pm 0.05$ and the transition temperature $T_c = 0.435$.

Figure 3(a) displays the simulation results of heat capacity and ΔU as a function of temperature for the case $J_1 = 1.0$, $J_2 = 0.67$, and $J_3 = 2.1$. In addition to the major anomalies, both the heat-capacity and ΔU data show broad humps around $T = 1.0$. This indicates the existence of two separate transitions, namely, a higher temperature transition in which bond-orientational order is created from the disordered phase, followed by a lower temperature transition in which the herringbone order is also established. Similar results are obtained for the case $J_2 = 0.75$.

By increasing the coupling constant J_2 to 0.85 and 0.95, the broad humps disappear. The heat-capacity data display a fairly symmetric anomaly. The simulation results

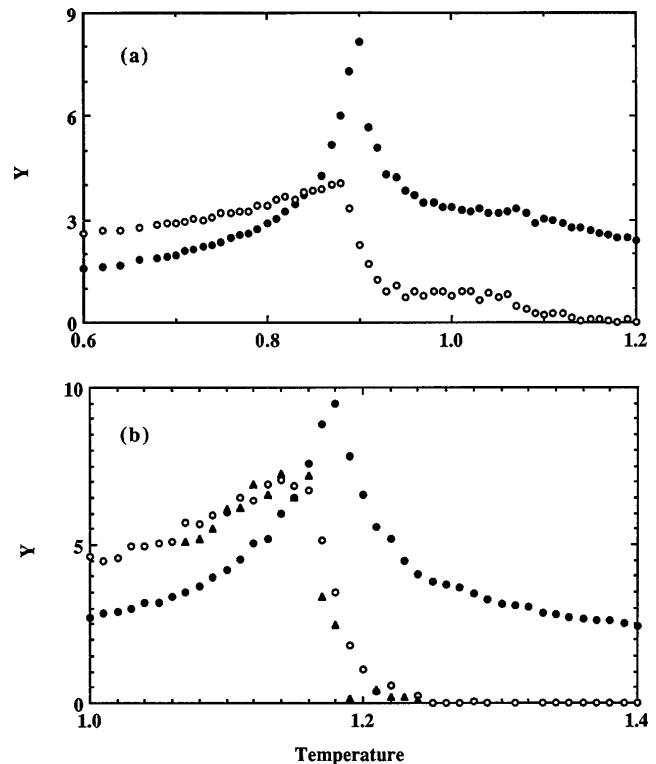


FIG. 3. Temperature variation of the heat capacity (solid dots) and the energy difference ($\Delta U/2$, open circles) for the cases of $J_2 = 0.67$ (a) and $J_2 = 0.95$ (b), respectively. For the case of $J_2 = 0.95$, simulation results for ΔU near the transition temperature from a significantly larger lattice (50×50) are shown as solid triangles.

using $J_2 = 0.95$ are shown in Fig. 3(b). As an important point, the ΔU data remain essentially zero in the disordered phase and exhibit a sharp rise in the immediate vicinity of the heat-capacity peak. No additional hump can be resolved near $T = 1.0$ from either the heat-capacity or ΔU data. This strongly suggests a single transition from the isotropic to the hexatic-herringbone phase. The nonzero values just above the heat-capacity peak position appear to be due primarily to finite-size effects. To confirm this hypothesis, simulations near the transition region were performed on a significantly larger lattice (50×50). These results are included in Fig. 3(b) as solid triangles. The width of the nonzero region immediately before the transition is clearly reduced for the larger lattice.

The helicity modulus calculated from the ΔU data is displayed in Fig. 4. It is clear that finite values for the helicity modulus are first obtained very near the peak position of the heat capacity. A simple power law fitting to the helicity data was found to yield $\nu = 0.82 \pm 0.05$; the fit is shown in Fig. 4 as the solid line. A similar value ($\nu = 0.81 \pm 0.05$) has been obtained for the case $J_2 = 0.85$. These results indicate that both bond-orientational and herringbone order can be simultaneously created

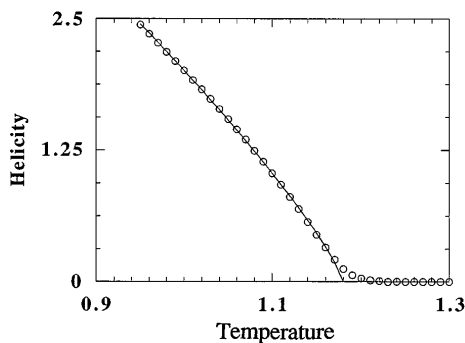


FIG. 4. Helicity modulus versus T . The solid line represents the simple power law fit result.

through a single continuous transition characterized by a distinct helicity modulus critical exponent.

Previously, by employing finite-size scaling analysis to the sharp heat-capacity anomaly observed, we have obtained the heat-capacity critical exponent ($\alpha = 0.36 \pm 0.05$) which is in good agreement with the exponent ($\alpha = 1/3$) characterizing the three-state Potts model in two dimensions [23]. However, the simple three-state Potts transition near $T = 0.43$ for $J_2 = 0.3$ is definitely different from the transition observed near $T = 1.17$ for $J_2 = 0.95$ which establishes both herringbone and hexatic order. Although the distinction is not readily apparent based on heat-capacity critical exponents, the helicity modulus critical exponents are clearly different, exhibiting the uniqueness of this novel transition. In light of this simulation result, analytic calculations of the Hamiltonian [Eq. (1)] near the single phase transition region are essential to gain further physical insight into the nature of this transition. In a two-dimensional liquid helium film, the helicity modulus is directly related to the superfluid density. Hopefully, by obtaining better physical insight into the stacked hexatic liquid-crystal phase found in *nmOBC* compounds, the calculated helicity modulus will be shown to be related to some measurable quantities.

The experimental determination of another critical exponent associated with the *SmA-HexB* transition of two-layer *nmOBC* films would also provide great insight into the nature of this transition. However, to the best of our knowledge, no such critical exponent is readily accessible. Even though it is a very difficult task, in light of this simulation work, high-resolution experimental characterization of the range of the herringbone order in the hexatic-*B* phase of *nmOBC* becomes very important.

We are grateful to Professor C. Campbell, Professor C. Dasgupta, Professor M. Schick, Professor K. Y. Szeto, and Professor J. Toner for valuable discussions. This work was supported by the National Science Council, Taiwan, under Contract No. NSC 82-0208-M-110-072, the Supercomputer Institute, University of Minnesota, and National Science Foundation, Solid State Chemistry, Grant No. DMR 93-00781.

*To whom correspondence should be addressed. Electronic address: huang001@maroon.tc.umn.edu

- [1] T. Stoebe, C.C. Huang, and J.W. Goodby, *Phys. Rev. Lett.* **68**, 2944 (1992); T. Stoebe and C.C. Huang (unpublished).
- [2] T. Stoebe and C.C. Huang, *Phys. Rev. E* **49**, 5238 (1994).
- [3] T. Stoebe, I.M. Jiang, S.N. Huang, A.J. Jin, and C.C. Huang, *Physica (Amsterdam)* **205A**, 108 (1994).
- [4] B.I. Halperin and D.R. Nelson, *Phys. Rev. Lett.* **41**, 121 (1978).
- [5] A.P. Young, *Phys. Rev. B* **19**, 1855 (1979).
- [6] T. Stoebe, J.T. Ho, and C.C. Huang, *Int. J. Thermophys.* **15**, 1189 (1994); A.J. Jin, M. Veum, T. Stoebe, C.F. Chou, J.T. Ho, S.W. Hui, V. Surendranath, and C.C. Huang, *Phys. Rev. E* (to be published).
- [7] M. den Nijs, *Phys. Rev. Lett.* **66**, 907 (1991); E. Granato, J.M. Kosterlitz, J. Lee, and M.P. Nightengale, *ibid.* **66**, 1090 (1991); M. den Nijs, *Phys. Rev. B* **46**, 10386 (1992).
- [8] R. Pindak, D.E. Moncton, S.C. Davey, and J.W. Goodby, *Phys. Rev. Lett.* **46**, 1135 (1981).
- [9] C.C. Huang, S.M. Viner, R. Pindak, and J.W. Goodby, *Phys. Rev. Lett.* **46**, 1289 (1981).
- [10] R. Bruinsma and G. Aeppli, *Phys. Rev. Lett.* **48**, 1625 (1982).
- [11] The x-ray diffraction [7] from thick 65OBC films first reveals the existence of the herringbone order in the *HexB* phase.
- [12] C.C. Huang, T. Stoebe, *Adv. Phys.* **42**, 343 (1993).
- [13] The tricritical point is a very special thermodynamic point in the T (temperature) and x (nonordering parameter) space. Thus it is extremely unlikely to have a tricritical line in the T -concentration space which represents the binary mixture systems.
- [14] K. Binder, in *Monte Carlo Methods in Statistical Physics*, edited by K. Binder (Springer, Berlin, 1979).
- [15] I.M. Jiang, S.N. Huang, J.Y. Ko, T. Stoebe, A.J. Jin, and C.C. Huang, *Phys. Rev. E* **48**, R3240 (1993).
- [16] M.E. Fisher, M.N. Barber, and D. Jasnow, *Phys. Rev. A* **8**, 1111 (1973).
- [17] We are conducting detailed helicity modulus simulations of the simple 2D *XY* model. The preliminary results from a 100×100 lattice clearly display a jump in helicity modulus near the Kosterlitz-Thouless transition temperature.
- [18] J.E. Van Humbergen and S. Chakravarty, *Phys. Rev. B* **23**, 359 (1981).
- [19] C. Bowen, D.L. Hunter, and N. Jan, *J. Stat. Phys.* **69**, 1097 (1992).
- [20] P. Olsson and P. Minnhagen, *Phys. Scr.* **43**, 203 (1991).
- [21] G. Ramirez-Santiago and J.V. Jose, *Phys. Rev. B* **49**, 9567 (1994).
- [22] R. Gupta, J. DeLapp, G.G. Batrouni, G.C. Fox, C.F. Baillie, and J. Apostolakis, *Phys. Rev. Lett.* **61**, 1996 (1988).
- [23] B. Nienhuis, A.N. Berker, E.K. Riedel, and M. Schick, *Phys. Rev. Lett.* **43**, 737 (1979).
- [24] In the three-state Potts transition, the transition temperature (T_c) is related to the energy difference between two energy states (ΔE), namely, $T_c = \Delta E/1.005$. In our model, $\Delta E = 3J_2/2$, thus $T_c = 3J_2/(2 \times 1.005)$.